

Contents

Chinese Abstract.....	I
English Abstract.....	IV
Acknowledges.....	VII
Contents.....	VIII
Table Captions.....	XII
Figure Captions.....	XIII

Chapter 1 Introduction

1-1 Introduction.....	1
1-2 Motivation for the study.....	7
1-3 Thesis Organization.....	8



Chapter 2 Literature review

2-1 structure of ferroelectric oxides.....	10
2-2 The composition of ferroelectrics.....	12
2-3 Fabrication methods of the ferroelectric thin films.....	15
2-4 Precursor solution of the ferroelectrics.....	17
2-5 Annealing atmosphere of the ferroelectrics films.....	23
2-6 Electrodes of the ferroelectric films.....	25
2-7 Sizes effects and thickness effect.....	26
2-8 Electrical properties of ferroelectric oxides.....	27
2-9 Reliability of ferroelectric films.....	32

Chapter 3 Experimental Details

3-1 Preparation of SBT, BNT, STO, STSO precursor solutions.....	38
3-2 Preparation of bottom electrodes.....	40
3-3 Formation of SBT, BNT, STO, STSO thin films.....	41
3-4 X-ray diffraction analysis (XRD).....	43
3-5 DTA and TG measurements.....	43
3-6 SEM measurement.....	44
3-7 TEM measurement.....	44
3-8 AFM measurement.....	45
3-9 XPS measurement.....	45
3-10 Polarization measurement.....	45
3-11 Capacitance-Voltage (C-V) measurements.....	46
3-12 Current-Voltage (I-V) measurements.....	47
3-13 Fatigue measurements.....	47
3-14 Retention measurements.....	48

Chapter 4 Electrical and Physical Properties of

$\text{Sr}_{0.8}\text{Bi}_{2+x}\text{Ta}_2\text{O}_{9+\delta}$ Ferroelectric Thin Films

4-1 Introduction.....	49
4-2 Experimental.....	49
4-3 Result and Discussion.....	51
4-4 Summary.....	64

Chapter 5 Electrical and dielectric properties of

low-temperature crystallized $\text{Sr}_{0.8}\text{Bi}_{2.6}\text{Ta}_2\text{O}_{9+x}$ thin films

5-1 Introduction.....	65
-----------------------	----

5-2 Experimental.....	66
5-3 Result and Discussion.....	67
5-4 Summary.....	78

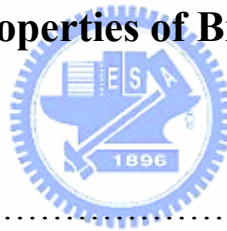
Chapter 6 Properties of $\text{Sr}_{0.8}\text{Bi}_{2.6}\text{Ta}_2\text{O}_{9+x}$ ferroelectric thin films with SrTiO_3 seeding layer on MIM and MFIS structure

structure

6-1 Introduction.....	80
6-2 Experimental.....	82
6-3 Result and Discussion.....	83
6-4 Summary.....	97

Chapter 7 Electrical Properties of $\text{Bi}_{3.25}\text{Nd}_{0.75}\text{Ti}_3\text{O}_{12}$ ferroelectric thin films

ferroelectric thin films



7-1 Introduction.....	99
7-2 Experimental.....	100
7-3 Result and Discussion.....	102
7-4 Summary.....	112

Chapter 8 Dielectric and Electrical properties of $\text{SrTiO}_{3-x}\text{SiO}_2$ thin film-based MIM capacitors

$\text{SrTiO}_{3-x}\text{SiO}_2$ thin film-based MIM capacitors

8-1 Introduction.....	114
8-2 Experimental.....	116
8-3 Result and Discussion.....	117
8-4 Summary.....	135

Chapter 9 Conclusions and Suggestions for Future Work

9-1 Conclusions.....137
9-2 Future work.....138
Reference.....140
Vita.....155



Table Captions

Chapter 1

Table 1-1. Comparison of memory IC.....2

Chapter 2

Table.2-1 Thin Film Deposition Techniques.....16

Chapter 3

Table 3-1 Calculated XRD data for SBT.....44

Chapter 5

Table 5-1 The composition and XRD grain size of SBT thin films
annealed at various temperatures.....71



Figure Captions

Chapter 1

Fig.1-1 Simple model of various FeRAM (a) 1T-1C type FeRAM (b) MFS (c) MFIS (d) MFMIS in FET-type FeRAM, respectively.....	3
--	---

Chapter 2

Fig. 2-1 The perovskite structure.....	11
Fig.2-2 The Bi-base layered perovskite structure of SBT (SBN).....	12
Fig.2-3 The P-E hysteresis curve of SBT(x/y/2)/Pt/Ti and SBT(x/y/2)/Pt/Ta films.....	13
Fig.2-4 The P-E curve (hysteresis loop) of SBT thin films.....	28
Fig.2-5 Illustration of the polarization reorientation.....	29
Fig.2-6 The four various mechanisms of polarization.....	31
Fig.2-7 A typical P-E hysteresis loop for ferroelectric.....	34
Fig.2-8 Time dependent dielectric breakdown.....	36
Fig.2-9 The operation of MFMIS FET.....	37

Chapter 3

Fig.3-1 The preparation of the precursors solution.....	39
Fig.3-2 The preparation of SBT thin films.....	42
Fig.3-3 The schematic circuit of Sawyer-Tower Bridge.....	46
Fig.3-4 Electrical measurement on MIM and MFMIS structure.....	47

Chapter 4

Fig.4-1 DTA and TG curves of the dried powder obtained from the precursor solution.....	51
Fig. 4-2 XRD patterns of the various bismuth content $\text{Sr}_{0.8}\text{Bi}_{2+x}\text{Ta}_2\text{O}_{9+\delta}$ thin films.....	52
Fig. 4-3 Lattice constant of $\text{Sr}_{0.8}\text{Bi}_{2+x}\text{Ta}_2\text{O}_{9+\delta}$ films as a function of excess bismuth.....	53
Fig. 4-4 SEM micrographs for 650 °C, 30 min sintered $\text{Sr}_{0.8}\text{Bi}_{2+x}\text{Ta}_2\text{O}_{9+\delta}$ thin film with various excess bismuth content indicated.....	54
Fig. 4-5 Bi XPS signals of SBT films with various excess bismuth contents.....	56
Fig. 4-6 P-E hysteresis loops of 650 °C, 30 min sintered $\text{Sr}_{0.8}\text{Bi}_{2+x}\text{Ta}_2\text{O}_{9+\delta}$ thin films with varying excess bismuth x.....	57
Fig. 4-7 Leakage current density vs. applied electric field for $\text{Sr}_{0.8}\text{Bi}_{2+x}\text{Ta}_2\text{O}_{9+\delta}$ thin films with various excess bismuth indicates.....	58
Fig. 4-8 Fatigue characteristics of SBT thin films with various excess bismuth contents annealed at 650 °C under 5V bipolar switching cycles.....	59
Fig. 4-9 (a) The TEM image of SBT thin film with excess bismuth 50% (x=1) (b) EDS spectra acquired from minor second phase (marked as black circle in TEM picture) of SBT thin film.....	60
Fig. 4-10 (a) SIMS depth profiles of SBT thin films as-deposited	61
Fig 4-10 (b) SIMS depth profiles of SBT thin films annealed at 650 °C, for 30 min.....	62

Fig 4-10 (c) SIMS depth profiles of SBT thin films annealed at 700 °C, for 30 min.....62

Fig. 4-11 Ln (J/E) is plotted versus $E^{1/2}$ for SBT films with various excess bismuth contents.....63

Fig. 4-12 Ln (J/E) is plotted versus $E^{1/2}$ for SBT films with Bi excess $x=1$64

Chapter 5

Fig. 5-1 (a) TEM cross section micrograph (b) SEM cross section micrographs of SBT thin film annealed at 450 °C and 550 °C, respectively.....68

Fig. 5-2 XRD pattern of SBT thin films (a) annealed at various temperatures indicated with 30 kV, 20 mA radiation and (b) annealed at 450 °C with 50 kV, 200 mA radiation.....69

Fig. 5-3 P-E hysteresis loops of SBT thin films annealed at various temperatures.....71

Fig. 5-4 Variation of dielectric constant of SBT thin films with annealing temperature.72

Fig. 5-5 SIMS depth profiles of SBT thin films annealed at (a) 650 °C, (b) 700 °C, for 30 min.....75

Fig. 5-6 Curves of leakage current density vs. applied electric field for SBT thin films annealed at various temperatures indicated.....76

Fig. 5-7 Variation of surface roughness and leakage current density at 100

kV/cm of SBT thin films with annealing temperature.....	77
Fig. 5-8 Fatigue characteristics of SBT thin films annealed at 650 and 700 under 5V bipolar switching cycles.....	78

Chapter 6

Fig. 6-1 XRD pattern of SBT thin films on Ir/SiO ₂ /Si substrate annealed at various temperatures.....	84
Fig. 6-2 XRD pattern of SBT thin films on STO/Ir/SiO ₂ /Si substrate annealed at various temperatures.....	85
Fig. 6-3 XRD pattern of SBT thin films deposited on (a) CeO ₂ /Si substrate and (b) with STO seeding layer annealed at 700	86
Fig. 6-4 SEM micrograph of SBT thin film (a) without STO seeding layer (b) with STO seeding layer on MFIS structure annealed at 700	87
Fig. 6-5 SEM cross section micrographs of SBT thin film (a) without STO seeding layer (b) with STO seeding layer on MFIS structure annealed at 700	87
Fig. 6-6 P-E hysteresis loops of SBT thin films without STO seeding layer on MIM structure annealed at 650 and 700	89
Fig. 6-7 P-E hysteresis loops of SBT thin films with STO seeding layer on MIM structure annealed at various temperatures.....	91
Fig. 6-8 C-V characteristic of the SBT thin films (a) without seeding layer and (b) with seeding layer on MFIS structure annealed at 700	92

Fig. 6-9 The leakage current density of the SBT thin films on MIM structure (a) without seeding layer (b) with seeding layer annealed at various temperatures, respectively.....94

Fig. 6-10 The leakage current density of the SBT thin films on MFIS structure (a) without seeding layer (b) with seeding layer annealed at 70095

Fig.6-11 Retention characteristics of SBT thin film in the MFIS structure with STO and without STO seeding layer annealed at 700 ..97

Chapter 7

Fig. 7-1 XRD pattern of BNT thin films annealed at various temperatures.103

Fig.7-2 SEM surface and cross section images of BNT thin film annealed at various temperature.....104

Fig. 7-3 P-E hysteresis loops of BNT thin films annealed at 650 and 700105

Fig. 7-4 Curves of leakage current density vs. applied electric field for BNT thin films annealed at 650 and 700106

Fig. 7-5 Fatigue characteristics of BNT thin films annealed at 700 under 5V bipolar switching cycles.....107

Fig.7-6 C-V characteristics of BNT thin film for Pt/BNT/Pt/Ti/SiO₂/Si (MFMIS) structure.....108

Fig.7-7 C-V characteristics of BNT thin film for

Pt/BNT/CeO ₂ /Pt/Ti/SiO ₂ /Si (MFMIS) structure.....	109
Fig.7-8 Relationship between MFM area-to-MIS area ratio and memory window.....	111
Fig.7-9 Retention characteristics of BNT thin film in the MFMIS structure.....	112

Chapter 8

Fig.8-1 XRD pattern of SrTiO ₃ thin films annealed at various temperatures.....	119
Fig.8-2 XRD patterns of SrTiSi _x O _{3±2y} thin films with various Si content as deposited at 400	119
Fig.8-3 XRD patterns of SrTiSi _x O _{3±2y} thin films with (a) x=0.25 and (b) x=0.45 as deposited at 400 and annealed at various temperatures.....	120
Fig.8-4(a) TEM electron diffraction pattern and (b) TEM micrograph of SrTiO ₃ thin films annealed at 800	122
Fig.8-4(c) TEM electron diffraction pattern and (d) micrograph of SrTiSi _x O _{3±2y} thin film with x=0.25 annealed at 800	123
Fig.8-5 SEM micrographs of surface morphology of SrTiO ₃ thin films (a) deposited at 400 and (b) annealed at 800	124
Fig.8-6 Surface and cross section SEM micrographs of SrTiSi _x O _{3±2y} thin film with x=0.25 (a) deposited at 400 and (b), (c) annealed at 800	125

Fig.8-7 Dielectric constant at zero bias versus SiO_2 mole ratio of $\text{SrTiSi}_x\text{O}_{3+\delta}$ thin film annealed at various temperatures indicated, the dash line and solid line was fitted with SiO_2 as dispersion phase by equation (1) and (2) , respectively.....126

Fig.8-8 Capacitance vs. applied voltage for SrTiO_3 thin film as deposited at 400 and annealed at various temperatures indicated.....129

Fig.8-9 Capacitance with applied voltage for $\text{SrTiSi}_x\text{O}_{3\pm 2y}$ thin film with $x=0.25$ annealed at various temperatures indicated.....130

Fig.8-10 Leakage current density of 100 kV/cm electric field vs. SiO_2 mol ratio of $\text{SrTiSi}_x\text{O}_{3\pm 2y}$ thin films annealed at various temperatures indicated.....132

Fig.8-11 XPS spectrum of the Si 2p 3/2 for the SrTiO_3 thin film with $x=0.25$ deposited at 400 and annealed at 800133

Fig.8-12 Curves of leakage current density vs. applied voltage for $\text{SrTiSi}_x\text{O}_{3\pm 2y}$ thin film with $x=0.25$ annealed at various temperatures indicated.....134

Fig.8-13 Time-dependent dielectric breakdown for $\text{SrTiSi}_x\text{O}_{3\pm 2y}$ thin film with $x=0.25$ annealed at 700 and 800135